


Article

# Climate-Growth Relations of *Abies georgei* along an Altitudinal Gradient in Haba Snow Mountain, Southwestern China

Mei Sun, Jianing Li , Renjie Cao, Kun Tian, Weiguo Zhang, Dingcai Yin and Yun Zhang \*

National Plateau Wetlands Research Center, Southwest Forestry University, Kunming 650224, China; sm0510215@163.com (M.S.); lijianing0411@163.com (J.L.); mrjie8488@163.com (R.C.); tlkunj@126.com (K.T.); zhangweiguo61@163.com (W.Z.); yindingcai@126.com (D.Y.)

\* Correspondence: zhangyuncool@163.com; Tel.: +86-1362-9670-659

**Abstract:** Climate warming has been detected and tree growth is sensitive to climate change in Northwestern Yunnan Plateau. *Abies georgei* is the main component of subalpine forest in the area. In this study, *A. georgei* ring width chronologies were constructed at four sites ranging from 3300 to 4150 m a.s.l. in Haba Snow Mountain, Southeastern edge of Tibetan Plateau. We analyzed the relationship between four constructed chronologies and climatic variables (monthly minimum temperature, monthly mean temperature, monthly maximum temperature, monthly total precipitation, the Standardized Precipitation-Evapotranspiration Index, and monthly relative humidity) by using response function analysis, moving interval analysis, and redundancy analysis. Overall, the growth of *A. georgei* was positively affected by common climatic factors (winter moisture conditions, autumn temperature, and previous autumn precipitation). At low and middle-low sites, May moisture condition and previous December precipitation controlled its radial growth with positive correlations. At middle-high and high sites, previous November temperature was the key factor affecting tree growth. The result of moving interval analysis was consistent with correlation analyses, particularly for May moisture at low altitudes.

**Keywords:** tree-ring; climate change; growth response; radial growth; Hengduan Mountain; Northwestern Yunnan Plateau



**Citation:** Sun, M.; Li, J.; Cao, R.; Tian, K.; Zhang, W.; Yin, D.; Zhang, Y. Climate-Growth Relations of *Abies georgei* along an Altitudinal Gradient in Haba Snow Mountain, Southwestern China. *Forests* **2021**, *12*, 1569. <https://doi.org/10.3390/f12111569>

Academic Editor: Warren Keith Moser

Received: 26 September 2021  
Accepted: 11 November 2021  
Published: 15 November 2021

**Publisher's Note:** MDPI stays neutral with regard to jurisdictional claims in published maps and institutional affiliations.



**Copyright:** © 2021 by the authors. Licensee MDPI, Basel, Switzerland. This article is an open access article distributed under the terms and conditions of the Creative Commons Attribution (CC BY) license (<https://creativecommons.org/licenses/by/4.0/>).

## 1. Introduction

Effects of climate change on forest ecosystems have been widely concerned [1–3], particularly for those forests at high altitudes where trees are more susceptible to climate warming [4,5]. Climate change directly affects tree regeneration, growth, and migrating abilities, and consequently influences forest dynamics [6–8]. Tree rings often contain an amount of climate information and have long been used as a valid tool to detect long-term climate-growth relationships [9,10], and to further evaluate future impacts of climate change on forest ecosystems [11,12].

Altitude is an important ecological factor, which often causes the redistribution of hydrothermal conditions affecting the tree radial growth [13]. It is generally believed that the radial growth is mainly affected by temperature in high altitudinal areas, while moisture conditions control tree growth at low altitudes [14,15]. However, due to the difference in the rate of climate change along the altitudinal gradient, this rule is not applicable in all cases [16,17], some research has also showed that the same tree species respond consistently to climate variables at different altitudes [17]. Studying climate-growth relations across species distributional range could help to learn how tree growth responds to climates in an area, and therefore to better understand forest dynamics and formulate proper management strategies under climate change scenarios.

The central Hengduan Mountain (HM) is located in the Southeastern edge of Tibet Plateau, with a complex topography, vertical climate belts, rich forest resources, and small human disturbances, and is considered as a climate sensitive area where a warming trend

has been observed during the past decades ( $0.3\text{ }^{\circ}\text{C}/\text{decade}$ ) [18]. This provides excellent conditions for studying the altitudinal trend of climate-growth relationships [19,20]. In recent decades, dendrochronological techniques have been widely applied in detecting climate-growth responses of conifer species at different sites in HM. Like *Picea likiangensis*, *Picea brachytyla*, *Tsuga dumosa*, *Abies ernestii*, and *Abies georgei* in Baima Snow Mountain [21,22]. *P. brachytyla* in Meili Snow Mountain and Geza [23,24]. *A. georgei*, *P. likiangensis*, *Pinus densata*, and *Larix potaninii* in Shika Snow Mountain [12,25]. *P. likiangensis* and *T. dumosa* in Yulong Snow Mountain [26,27]. These studies showed that both temperature and precipitation influenced tree radial growth in HM, but growth response to climate varied with tree species and sites. Haba Snow Mountain (HSM) is a typical snow mountain in the central HM with a well-preserved forest ecosystem, however, little is known about impacts of climate change on tree growth in the area [28], particularly in altitudinal trends of climate-growth relationships. Recently, growth responses of *A. georgei* to climate factors at the upper distributional limit in HSM (data also used in this paper) has been detected [29].

*A. georgei* is a high-altitude conifer widely distributed in HM and is known as the main tree species compositing subalpine forests. Prior studies have revealed that higher temperatures in the previous November–December and current June–August stimulate the species radial growth at its upper distributional limit in HM [23,29], while current June and September precipitation limit its growth [29]. However, studies on climate-growth relationships of *A. georgei* along the altitudinal gradient in HM are rather scant [25]. Therefore, the aim of this study is to identify the main climatic factors influencing *A. georgei* growth at different altitudes in HSM and to evaluate the temporal stability of the climate-growth relationship. Given that high-altitudes with low temperature in HSM and temperature decrease as altitudes increase, we expect that *A. georgei* growth is temperature-limited and this sensitivity is more obvious at higher altitudes.

## 2. Materials and Methods

### 2.1. Study Area

Haba Snow Mountain (HSM) is located in the Northwestern Yunnan and the South-eastern edge of the Tibet Plateau (Figure 1). The highest point of HSM is 5396 m a.s.l., and the lowest point is 1550 m a.s.l. near beside Jinsha River. From the Jinsha River valley to the peak of HSM, different vertical climate zones are formed successively, such as the sub-tropical zone (1550–1800 m a.s.l.), northern subtropical zone (1800–2100 m a.s.l.), warm temperate zone (2100–2500 m a.s.l.), moderate temperate zone (2500–3100 m a.s.l.), cold temperate zone (3100–4100 m a.s.l.), cold zone (4100–4700 m a.s.l.), and permanent ice and snow zones (above 4700 m a.s.l.) [30,31]. The type of forest vegetation corresponding to the vertical climate zone has been formed. Below 2100 m a.s.l., the dry and warm river valleys is dominated by shrub species such as *Ziziphus mintana*, *Terinalia franchetii*, and *Caryopteris forrestii*. Between 2100 and 2850 m a.s.l., a warm and temperate coniferous forest is dominated by *Pinus yunnanensis* and *Pinus amandii*. From 2900 to 3200 m a.s.l., *P. densata* is the dominant species and formed a coniferous forest. At altitudes of 3300–4100 m a.s.l., it is a cold-temperate coniferous forest with *P. likiangensis*, *Larix potaninii*, and *A. georgei* as the major species. Altitudes above 4200 m a.s.l. are alpine meadows and alpine screes sparse vegetation [31].

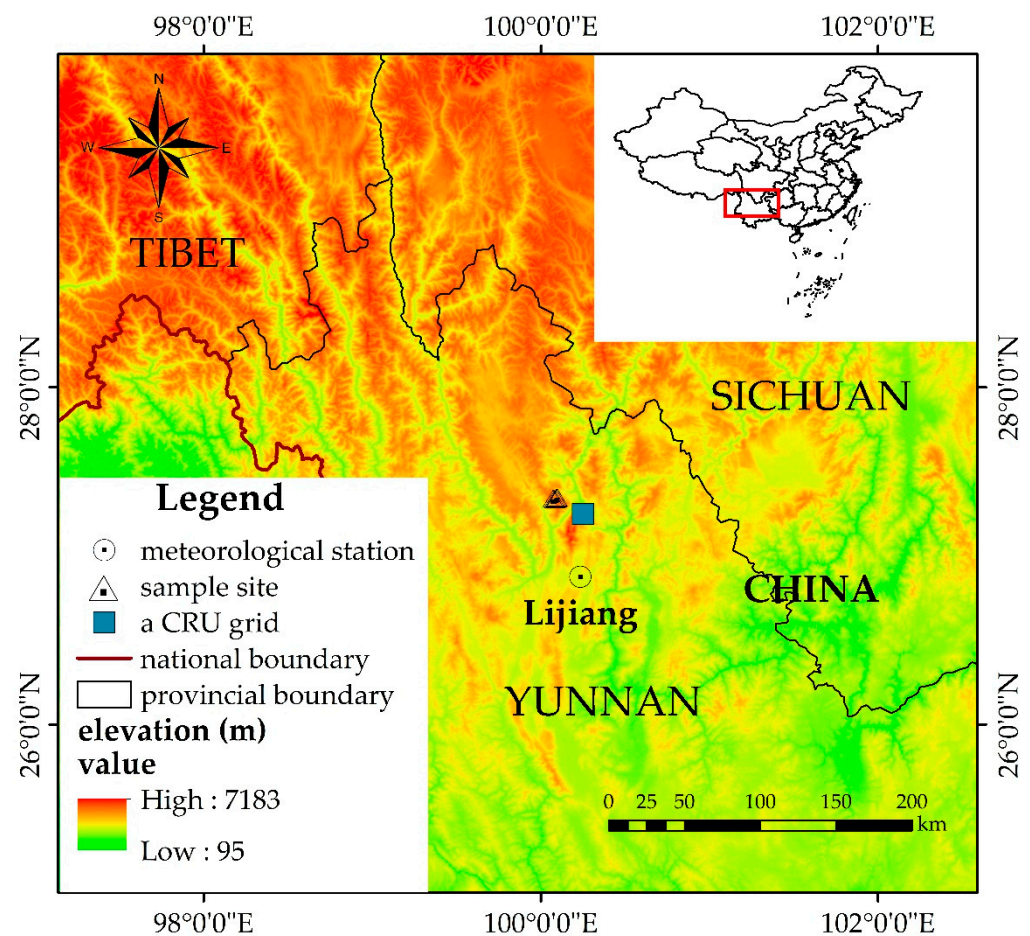


**Figure 1.** Location of the study area, the sampling site, and the meteorological station.

*A. georgei* is a shade-tolerant and shallow-rooted species, adapted to humid climate, and grown in the gray-brown forest soil, which is generally founded at altitudes of 3200–4100 m a.s.l. According to the results of the “Comprehensive Scientific Investigation of the Haba Snow Mountain Nature Reserve in Yunnan”, the total forest area is 11,391.8 hm<sup>2</sup>, while the *A. georgei* forest area is 4121.7 hm<sup>2</sup>, accounting for 36.18% of the total forest area.

The HSM is affected by a South-Asian monsoon climate, which is characterized by distinct wet and dry seasons [31]. According to the climate data of 1951–2016 from the Lijiang meteorological station (Figure 2), the annual average temperature is 12.9 °C, the coldest in January with an average temperature of 6.2 °C, and the hottest in June with an average temperature of 18.2 °C. The average annual precipitation is 959.37 mm. The precipitation is mainly concentrated in the rainy season (June–October). The precipitation is 842.40 mm, accounting for 87.81% of the annual precipitation.

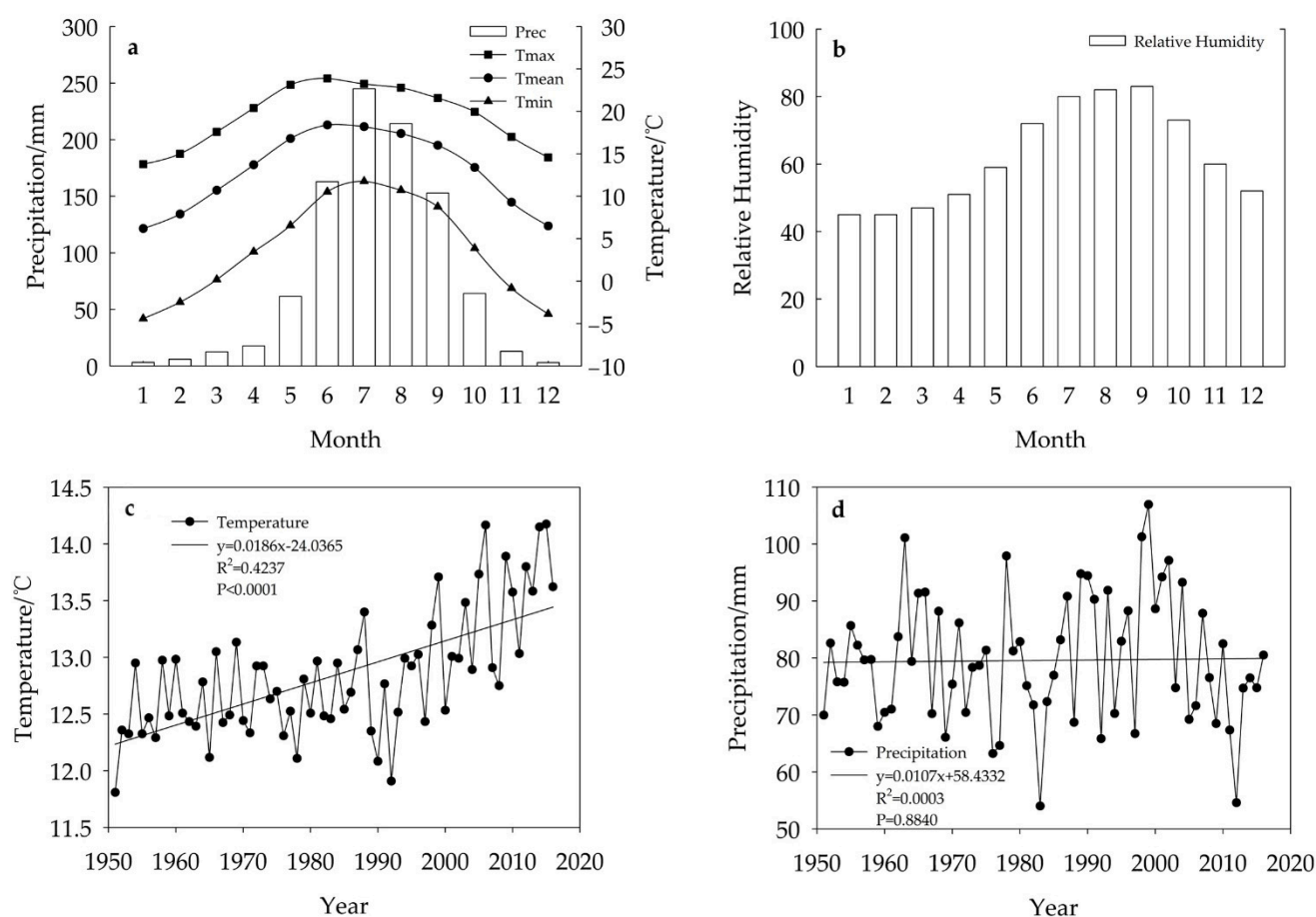


**Figure 2.** Climate data from the Lijiang meteorological station (1951–2016). Monthly minimum temperature ( $T_{\min}$ ), monthly mean temperature ( $T_{\text{mean}}$ ), monthly maximum temperature ( $T_{\max}$ ), and total precipitation (Prec) (a). Relative humidity (b). Trends of annually mean temperature (c). Trends of annually total precipitation (d).

## 2.2. Tree-Ring Sampling and Chronology Development

In 2017, we collected tree-ring samples at four altitudes (3317 m, 3682 m, 3967 m, and 4152 m), spanning the altitudinal distributional range of *A. georgei*. When sampling, large, healthy, and undisturbed trees were selected. After sampling, we used a branch to block the hole caused by drilling to prevent insects entering, which may be helpful for wound securing and avoiding diseases. For each tree, two cores parallel to the contour line at breast height were taken. We placed the obtained cores into a plastic straw and numbered them. The altitude deviation was controlled within 10 m at each altitude to keep the consistency of climatic signal. In total, 128 trees and 230 cores were collected at four altitudes (Table 1).

**Table 1.** The information of sampling sites.

Sites	Altitude/m a.s.l.	Longitude/E	Latitude/N	No. (Tree/Core)
Low altitude (L)	3317	100°04′54.78″	27°20′19.86″	26/52
Middle–Low altitude (ML)	3682	100°04′19.62″	27°20′25.37″	33/60
Middle–High altitude (MH)	3967	100°05′31.25″	27°20′39.71″	35/62
High altitude (H)	4152	100°05′51.48″	27°20′48.90″	34/56

The samples were brought back to the laboratory and were treated in accordance with the standard process of dendrochronological techniques [32]. After the samples were naturally air-dried, they were fixed and polished. Each core was placed under a binocular microscope for preliminary dating, and then scanned at high resolution (2400 dots per inch) on an EPSON Scan (Expression 11000XL, Seiko Epson Corporation, Nagano, Suwa, Japan) scanner. Ring widths on each scanned image were measured at an accuracy of 0.001 mm by using the software CooRecorder version 9.3 and cores from the same tree were cross-dated by using the software CDendro version 9.3 [33]. Dating results of ring width series were checked by using the program COFECHA [34]. The cores that had low correlations with the main sequence were eliminated. Finally, 124 trees and 216 cores remained and were selected for next analysis.

To maximally retain the climatic signals, ring width measurements were developed by using the ARSTAN program [34]. Ring-width series were standardized to remove the biological growth trend, as well as any other low-frequency variations induced by stand dynamics. The detrending procedure assumed a 50% frequency response over a 100-year frequency band. This detrending method allows maximizing the common signals among individual tree-ring series. To reduce the influence of outliers in the computation of the mean chronologies, all detrended series were averaged on a site-by-site basis by using the bi-weight robust mean. Residual chronologies were produced to remove any auto-correlation effects and were used for further analyses. The quality of chronologies was evaluated by several statistics, such as mean sensitivity, signal-to-noise ratio, and expressed population signal.

### 2.3. Climate Data

We collected monthly minimum temperature, monthly mean temperature, monthly maximum temperature, monthly precipitation, and relative humidity in the period between 1951 and 2016 from the Lijiang meteorological station (27°50' N, 99°42' E, 3276.7 m). To further detect the effect of moisture condition on tree growth, the Standardized Precipitation-Evapotranspiration Index (SPEI) [35] was also applied and datasets (1951–2016) were obtained from a CRU grid (CRUTS4.03, <https://spei.csic.es/database.html> (accessed on 11 November 2021)).

### 2.4. Climate-Growth Relationships

Since climate has a lagging effect on tree growth [36], climate variables from previous September to current October were selected for the correlation analysis by using program DendroClim2002 [37]. To detect accumulation effects of climate on tree growth, we also selected seasonal data, i.e., the post-growing season (September–October) of the previous year, the dormant season (January–March), the early growing season (April–May), the growing season (June–August), and the post-growing season of the current year. The response function first extracts the principal component of the climate variables and then performs regression analysis, which can more accurately reflect the extent to sample data affected by environmental factors. Therefore, we use correlation coefficients of the response function to reflect the relationship between tree growth and climate factors.

We also assessed the temporal stability of climate-growth relationships by using evolutionary and moving response functions module in DendroClim2002. Evolutionary intervals were calculated using forward and backward selection with a window period of 22 years.

To further explore climate-growth relationships, we applied redundancy analysis (RDA) by using the program CANOCO4.5 [38]. In RDA correlation matrix, residual chronologies were the response variables, years were the samples, and climate variables were the explanatory variables. Significant ( $p < 0.05$ ) climate variables were selected after applying forward selection using a Monte Carlo permutation test based on 999 random permutations [38].



### 3. Results

#### 3.1. Tree-Ring Chronologies

The length of *A. georgei* residual chronology of the four sampling sites (Figure 3) increased from low to high altitudes (Table 2). Each statistical characteristic value did not show a clear trend along the altitudinal gradient, but all had higher mean sensitivity (MS) and higher expressed population signal (EPS) with a value above 0.90, indicating that the chronologies had a high quality and could represent the characteristics of tree-ring width in the area, and that they could be used in this dendrochronological study. Tree-ring chronologies from adjacent sites showed significant and positive correlations over the common period 1951–2016 (Table 3), indicating the similarity in the growth sensitivity to climate signals at four altitudes.

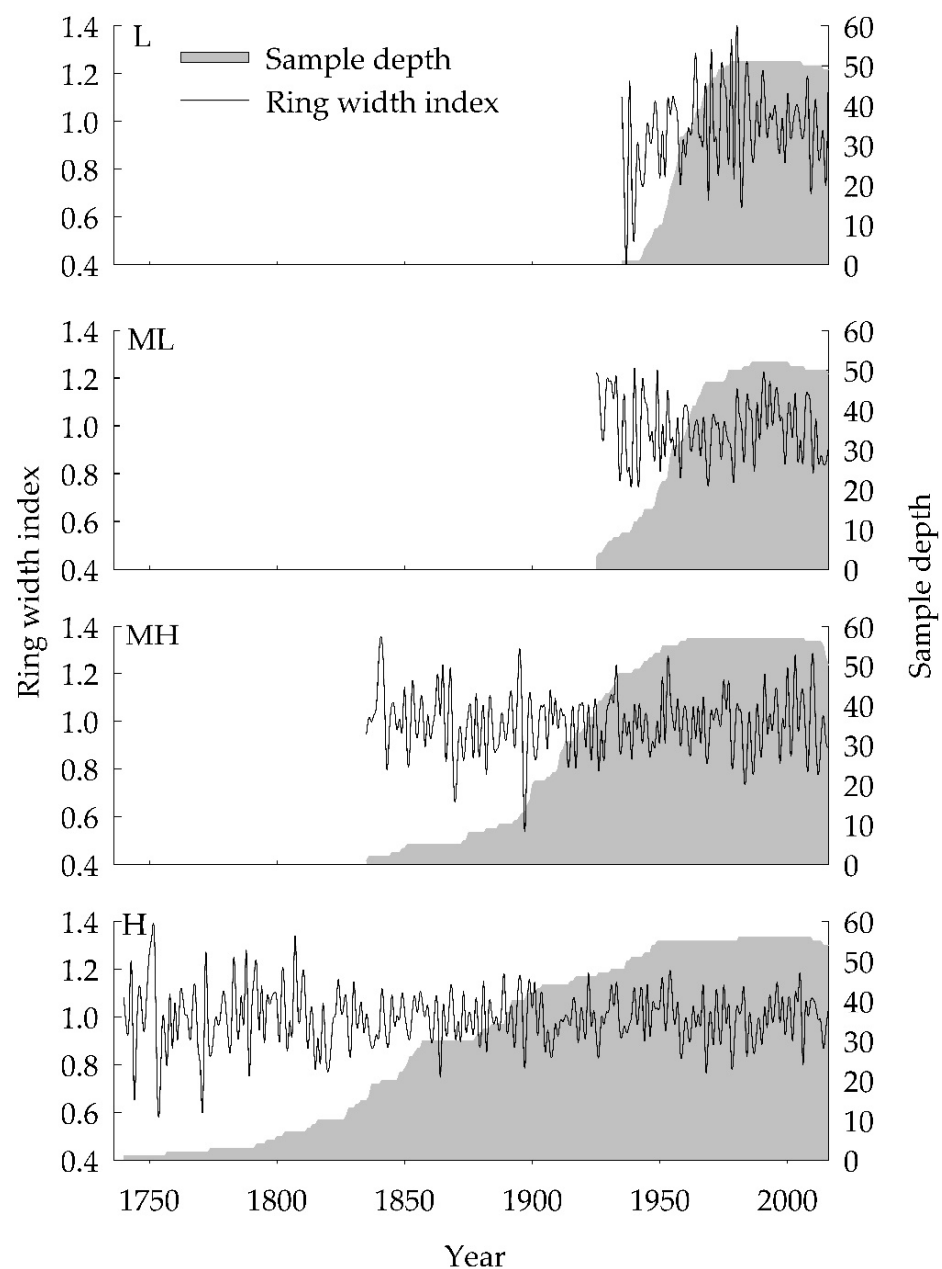


**Figure 3.** Residual chronologies and sample depth at four altitudes. The residual chronology of low altitude (L). The residual chronology of Middle-Low altitude (ML). The residual chronology of Middle-High altitude (MH). The residual chronology of High altitude (H).

**Table 2.** Statistics of residual chronologies and common interval analysis.

Residual Chronologies	L	ML	MH	H
No. (tree/radii)	26/51	30/52	34/57	34/56
chronology length	1933–2016	1923–2016	1831–2016	1737–2016
Mean sensitivity	0.21	0.14	0.15	0.11
Statistics of common interval analysis (1950–2016)				
Variance in first eigenvector/%	49.33%	32.18%	34.79%	36.20%
Standard deviation	0.18	0.13	0.12	0.10
Signal-to-noise ratio	6.77	6.25	22.20	26.81
Expressed population signal	0.87	0.86	0.96	0.96

**Table 3.** Pearson correlation coefficients among four chronologies of *A. georgei* for the common period 1951–2016. Significance level: \*\*,  $p < 0.01$ .

	L	ML	MH	H
L	1.000			
ML	0.367 **	1.000		
MH	0.076	0.348 **	1.000	
H	0.027	0.363 **	0.494 **	1.000

### 3.2. Relationship between Ring width Index and Climate Variables

The results of response function (Figure 4) showed that the radial growth of *A. georgei* at low altitudes (L and ML) was more affected by moisture condition than temperature. May moisture availability was consistent at both L and ML, by showing negative correlations with  $T_{\text{mean}}$  and  $T_{\text{max}}$  (Figure 4a) and positive correlations with humidity (Figure 4b). At L, previous October and December precipitation and SPEI, and current June relative humidity and SPEI positively influenced tree growth. While precipitation in previous October and current January positively affected tree growth at ML. At high altitudes (MH and H), the radial growth of *A. georgei* was significantly and positively correlated with the previous November temperature.

For the result of seasonal analysis, moisture condition before current growing season was important in tree growth at the L site, by showing significant correlations of precipitation, SPEI, and relative humidity with PPG, DG, and EG (Figure 4b), temperature negatively and positively affected tree growth in EG and PG, respectively (Figure 4a). At the ML site, temperature negatively influenced tree growth in EG, while relative humidity and precipitation positively affected tree growth in DG. No significant correlations were found at two high altitude sites.



Figure 4. Cont.



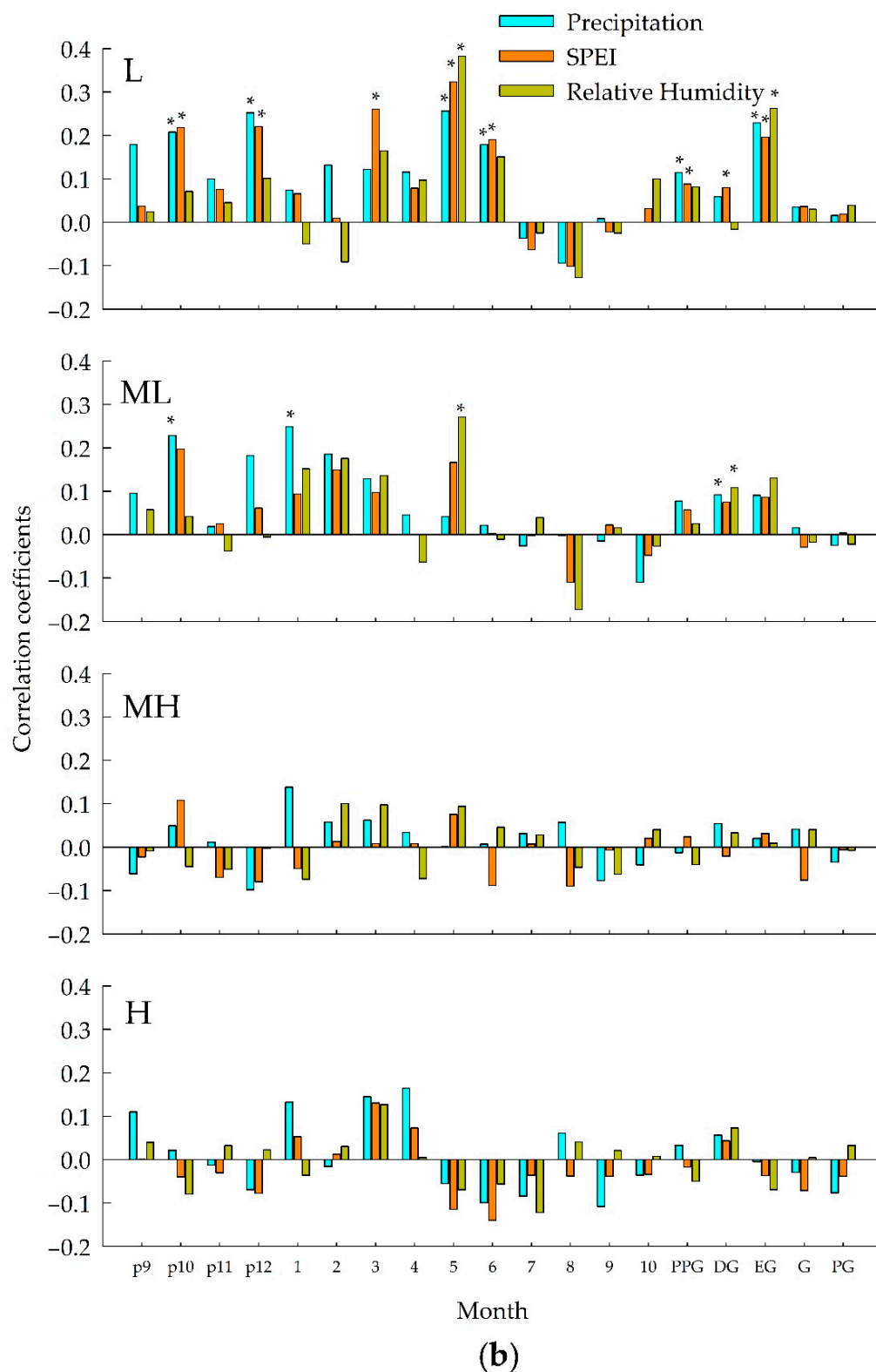


**Figure 4.** Relationships between residual chronologies and climatic factors. \*  $p < 0.05$ . Correlation coefficients of  $T_{\min}$ ,  $T_{\text{mean}}$  and  $T_{\max}$  computed by response function (a). Correlation coefficients of Prec, SPEI and relative humidity computed by response function (b). PPG indicates the previous post growing season (September–October); DG indicates the dormant season (January–March); EG indicates the early growing season (April–May); G indicates the growing season (June–August); PG indicates the post growing season (September–October); p indicates the previous year.

### 3.3. Dynamic Relationships between Radial Growth and Climatic Change

The climate-growth relationship (Table 4) was stable at the L site, particularly for May (temperature, precipitation, SPEI and relative humidity) by showing significant correlations at all years. For previous October and December precipitation, significant correlations were found at most years. The relationship of SPEI was more stable in previous December than in previous October and current March, by showing more significant years. The October temperature showed a quite stable relationship with tree growth by showing significant correlations in some years. At ML, significant correlations were found at all years for May temperature and most years for May relative humidity, January and previous October precipitation, indicating a stable relationship. The stability was good at MH by showing significant correlations at most studied years, while it was poor at H by showing several years with significant correlations.

**Table 4.** Analyses with moving intervals between the residual chronologies and the monthly climatic variables.

Sampling Site	Interval Period	Climatic Variable	Significant Year
L	1953–2016	Previous October precipitation	1953–1970 (+), 1974–1990 (+), 2012 (+), 2014–2016 (+)
		Previous December precipitation	1953–1985 (+), 1992–1993 (+), 1995 (+), 1999–2016 (+)
		Current May precipitation	1953–2016 (+)
		Previous October SPEI	1953–1963 (+), 1968–1969 (+), 1980 (+), 1993–2009 (+), 2014–2016 (+)
		Previous December SPEI	1953–1990 (+), 2002 (+), 2007 (+), 2009 (+), 2011 (+), 2013–2016 (+)
		Current March SPEI	1953–1965 (+), 1967 (+), 1969 (+), 1986–1987 (+), 1999 (+), 2002–2016 (+)
		Current May SPEI	1953–2016 (+)
		Current May relative humidity	1953–2016 (+)
		Current May temperature	1953–2016 (–)
		Current October temperature	1953–1967 (+), 1972–1976 (+), 1998 (+), 2000–2001 (+), 2003–2013 (+), 2015–2016 (+)
ML	1953–2016	Previous October precipitation	1953–1963 (+), 1966–1967 (+), 1980–1986 (+), 1990–1994 (+), 2006–2007 (+), 2009–2016 (+)
		Current January precipitation	1953–1969 (+), 1973–1975 (+), 1989–1990 (+), 2003 (+), 2006–2016 (+)
		Current May relative humidity	1953–1970 (+), 1972–1975 (+), 1978 (+), 1980–1985 (+), 2004 (+), 2007–2016 (+)
		Current May temperature	1953–2016 (–)
MH	1953–2016	Previous November temperature	1953–1967 (+), 1974 (+), 1980–1981 (+), 1983–1996 (+), 2000 (+), 2003 (+), 2011–2016 (+)
H	1953–2016	Previous November temperature	1953–1965 (+), 2014–2016 (+)

Note: (+) indicates a significant and positive correlation; (–) indicates a significant and negative correlation.

### 3.4. Redundancy Analysis between Climatic Factors and Residual Chronologies

According to RDA results (Figure 5), the moisture condition played a more important role in tree growth at low altitudes (L and ML), indicated by a smaller angle between their chronology vectors and moisture vectors (March and May relative humidity, and previous December precipitation) than two temperature vectors. Vice versa, tree growth was more affected by temperature at high altitudes (MH and H) by showing closer relationships with temperature in previous November and current September.

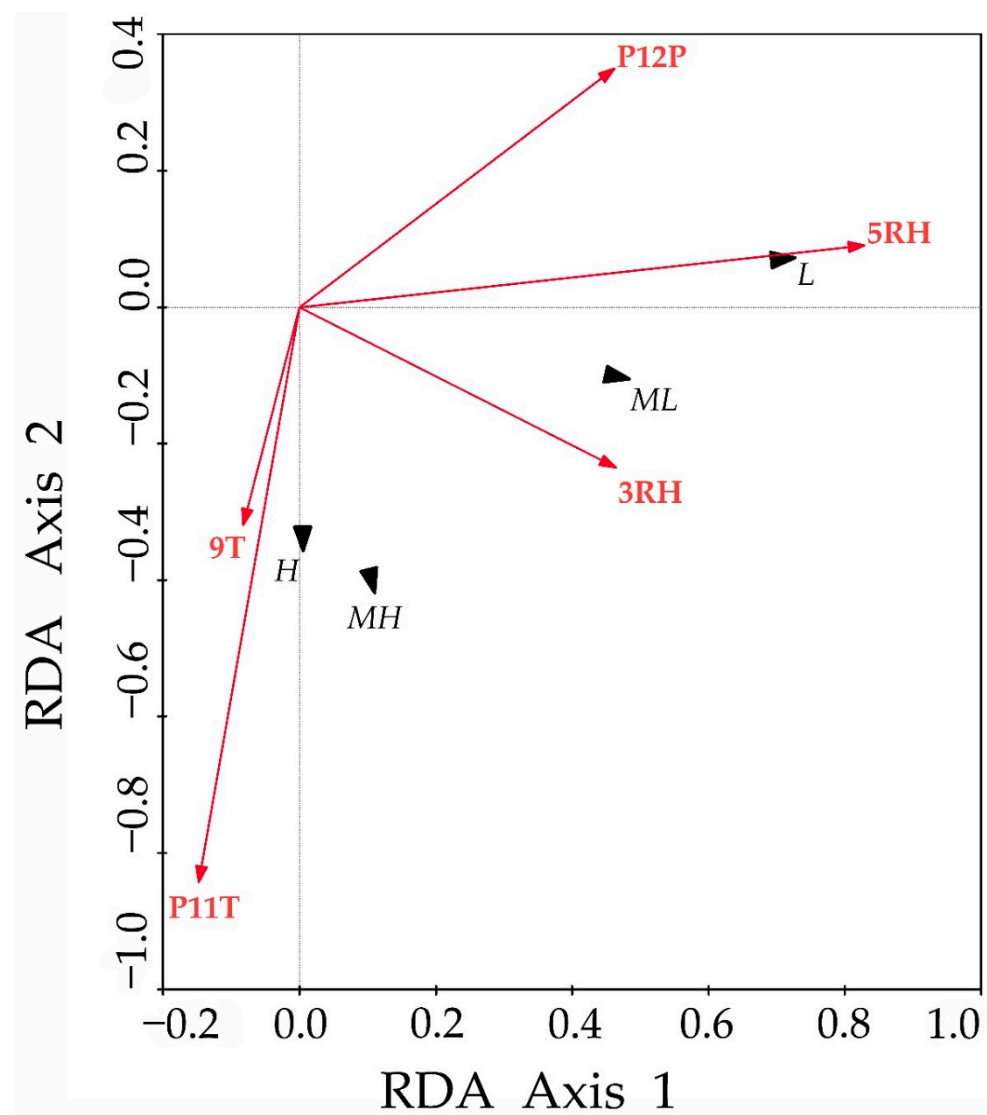


**Figure 5.** Redundancy analysis between climatic factors and residual chronologies (1951–2016). Only significant climatic factors ( $p < 0.05$ ) are shown. The longer vector of climate factor indicates the greater contribution; correlation coefficients between the climatic factors and the chronologies are illustrated by the cosine of the angle between the two vectors. Vectors pointing in the same directions indicate a positive correlation, and in opposite directions indicate a negative correlation. Numbers represent the corresponding months, T represents temperature; P represents precipitation; RH represents relative humidity. The letter P before number represents previous year. L indicates the residual chronology of low altitude; ML indicates the residual chronology of Middle–Low altitude; MH indicates the residual chronology of Middle–High altitude; H indicates the residual chronology of high altitude.

### 3.5. Altitudinal Trends of Growth Responses

The strength in responses of the May moisture condition decreased with increasing altitudes (Figure 6a). The effect of previous November temperature turned from negative to positive towards higher altitudes, while the impacts of an early growing season (negative) became weak as the altitude increased (Figure 6b). Previous December precipitation turned from positive to negative with increasing altitudes, while there was no significant trend in DG SPEI (Figure 6c). The coefficients of PPG precipitation decreased with increasing altitudes, but the trend was not significant (Figure 6d).

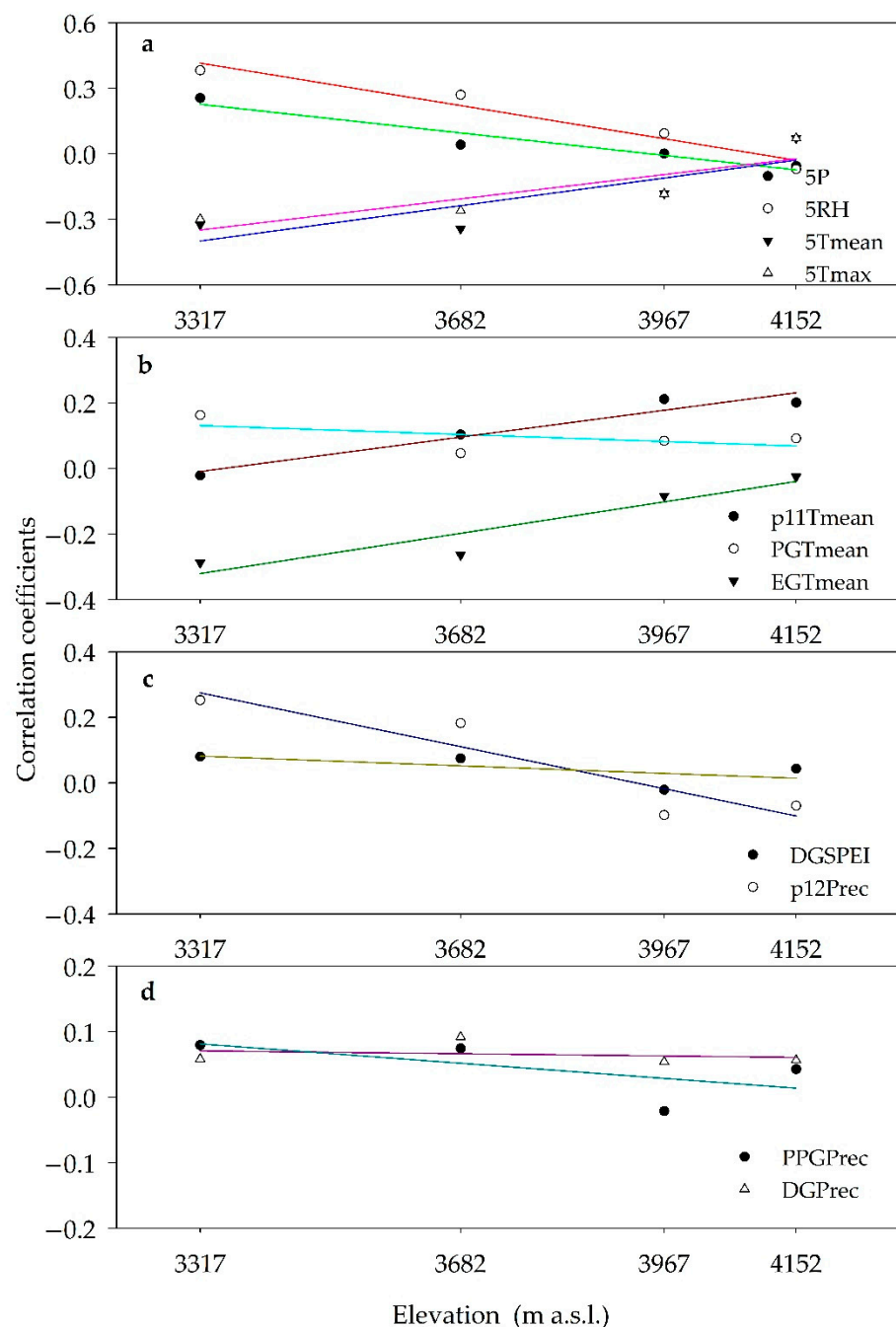


**Figure 6.** Altitudinal trends in correlation coefficients of *A. georgei* with significant climate factors between 1951 and 2016. May moisture condition (temperature, precipitation, and relative humidity) (a). Temperature (previous November, current early growing season, and post growing season) (b). Precipitation in previous December and SPEI in dormant growing season (c). Dormant growing season and previous post growing season (d).

#### 4. Discussion

Our results revealed that the radial growth of *A. georgei* was more affected by the moisture condition at a lower distributional range while by temperature at higher altitudinal sites in HSM, which supported one of our hypotheses that the strength of temperature impacts enhanced as altitude increased, but rejected another hypothesis that low temperature was the main factor controlling tree growth across the altitudinal distributional range. Consistent to our findings, the importance of moisture (temperature) decreased (increased) with increases in altitudes has been reported in nearby central Himalaya [39,40].

#### 4.1. Climate-Growth Relationships along the Altitudinal Gradient

May moisture condition is a dominant factor influencing the radial growth of *A. georgei* at low altitudes. Since May is relatively dry in the studied area with high temperature and low precipitation (Figure 2), *A. georgei* start growing and growth may suffer from drought stress due to insufficient water supply caused by increased plant transpiration and soil water evaporation [41], consequently limiting tree early growth. In addition, the soil in HSM is poor in water retention and holding capacity, which easily leads to drought stress when water is insufficient [30]. However, the temperature is lower with less evapotranspiration at high altitudes, therefore drought stress was not detected at high altitudinal sites. Similar results have also been reported in Southeastern Tibetan Plateau [42,43], Central Tibetan Plateau [44–46], and Western Himalayas [47].

More precipitation in previous December could enhance *A. georgei* growth at lower sites, since more precipitation in winter can provide higher water reserve availability for tree growth at the beginning of the growing season in the next year, particularly for those lower sites under May drought stress (as discussed in above paragraph). The positive effects of previous December precipitation on tree growth at the lower limit was also reported for *P. densata* at HSM [48]. However, it became weak (coefficients) and turned into negative correlation at higher sites, reflecting that precipitation was not limiting at the species upper distributional limit.

Previous November temperature was found to be important in determining tree growth at high altitudes. November is the season for dormant bud formation, if the temperature is too low, the number of dormant bud formation will be reduced [49,50]. Furthermore, low temperature would cause needle leaves die due to the leaf tissue frozen, thereby reducing photosynthesis production and restricting tree growth in the next year. The relationship turned into slightly negative (not significant) at the lowest site, the temperature was higher at the lower site, and the precipitation gradually became more important. Positive effects on subalpine tree growth were also reported at Central Austrian Alps and Slovakia [36,51].

#### 4.2. Consistent Effects among All Sites

Cambial activity is generally slow in the post growing season with low temperature [52,53], although September and October are in the post growing season and cambial activity is weak, high temperature can still promote the photosynthesis to produce nutrients for tree growth and extend the growing season, consequently forming wide ring width in the current year [45]. Similar results have been proved in conifer trees of neighboring areas [46,54].

The moisture condition during winter (January to March) positively affected tree growth. On the one hand, *A. georgei* is a shallow-rooted tree species, and the dormant season precipitation is mainly snowfall. Snowfall can form a thermal insulation layer on the ground, which can prevent the root system from being damaged by the low temperature during the winter, which is conducive to tree growth in the cold weather. The same conclusion has been reported for conifer trees at Tianshan Mountain in Northern China and high elevation sites in Northern Patagonia of Argentina [55,56]. On the other hand, snowfall during the dormant period is conducive to maintaining good soil moisture and increasing the water reserve in the early growing season [57]. The effects of winter snowfall on tree growth have the same results in previous studies, such as the subalpine in Northwestern Yunnan [26], the Northeastern subalpine in China [58], the subalpine in Central Japan [59], and Quebec [60].

Our results have revealed that precipitation during the previous post growing season (mainly October) is also a critical factor that positively affected tree growth across the altitudes, particularly at two low sites. Adequate precipitation in the post growing season of the last year would keep the soil in a good moisture condition and may increase the accumulation of carbohydrates, which is beneficial to tree growth of the coming year [61].

In addition, high temperatures in the early growing season had negative impacts on tree growth, suggesting that moisture conditions in spring was important for tree growth. Significant correlations only presented at two low sites (Figure 4a) and correlation coefficients decreased with increasing altitude (Figure 6b), the finding supported the result of May moisture condition impacts, indicating that drought stress was more obvious at low sites than at high sites.

#### 4.3. Temporal Stability in Climate-Growth Relationships

The stability by moving interval analysis supported the results of correlation analyses by response function and RDA. Those climatic factors with significant correlations of tree growth were presented at many time scales, particularly for May climatic conditions (temperature, precipitation, SPEI and relative humidity) at the L site, indicating the key effect of the May moisture condition on the species growth at low altitude. At the ML site, the negative effects of May temperature on tree growth was similar to site L, suggesting drought stress on tree growth at low altitudes. The stability of previous November temperature at MH and H site was relatively weak by showing less significant years as compared to other climatic factors, but it still proved the importance of temperature on the species radial growth at high altitude. There were no obvious increases in the years showing significant correlations since 1980s or 1990s, and it is likely that the warming may not reach the threshold to affect tree growth.

### 5. Conclusions

The radial growth of *A. georgei* responded differently to climates along the altitudinal gradient in HSM, generally showing moisture sensitivity at lower altitudes (L and ML sites) and temperature control at higher altitudes. Current May moisture condition and previous December precipitation played an important role in affecting tree growth at low altitudes, while the previous November temperature was the key factor at high altitudes. More precipitation in winter and early spring and higher temperature in the late growing season would stimulate tree growth in the area. The stability analysis supported the results of two correlation analyses, and it can provide more accuracy information for the understanding of the climate-growth relationship dynamics.

**Author Contributions:** M.S. finished the manuscript, J.L. and R.C. analyzed the data, K.T. put forward the idea of the article, D.Y. and W.Z. helped field sampling, Y.Z. modified the article. All authors have read and agreed to the published version of the manuscript.

**Funding:** This work was funded by the National Natural Science Foundation of China (31600395) and the Plateau Wetlands Science Innovation Team of Yunnan Province (2012HC007).

**Data Availability Statement:** The data presented in this study are available on request from the corresponding author.

**Acknowledgments:** We thank Lei Wang with help in improving the quality of the figures. We thank Raphael Chavardes and Igor Drobyshev for their continuous support throughout this project.

**Conflicts of Interest:** The authors declare no conflict of interest.

### References

1. Maes, S.L.; Perring, M.P.; Vanhellefont, M.; Depauw, L.; Verheyen, K. Environmental drivers interactively affect individual tree growth across temperate European forests. *Glob. Chang. Biol.* **2019**, *25*, 201–217. [[CrossRef](#)] [[PubMed](#)]
2. Boisvenue, C.; Running, S.W. Impacts of climate change on natural forest productivity-evidence since the middle of the 20th century. *Glob. Chang. Biol.* **2006**, *12*, 862–882. [[CrossRef](#)]
3. Hessburg, P.F.; Miller, C.L.; Povak, N.A.; Taylor, A.H.; Safford, H.D. Climate, Environment, and Disturbance History Govern Resilience of Western North American Forests. *Front. Ecol. Evol.* **2019**, *7*, 239. [[CrossRef](#)]
4. Galván, J.D.; Büntgen, U.; Ginzler, C.; Grudd, H.; Camarero, J.J. Drought-induced weakening of growth-temperature associations in high-elevation Iberian pines. *Glob. Planet. Chang.* **2015**, *124*, 95–106. [[CrossRef](#)]
5. Shi, C.; Shen, M.; Wu, X.; Cheng, X.; Li, X.; Fan, T.; Li, Z.; Zhang, Y.; Fan, Z.; Shi, F. Growth response of alpine treeline forests to a warmer and drier climate on the southeastern Tibetan Plateau. *Agric. For. Meteorol.* **2018**, *264*, 73–79. [[CrossRef](#)]



6. Lu, X.; Liang, E.; Wang, Y.; Babst, F.; Leavitt, S.W.; Camarero, J.J. Past the climate optimum: Recruitment is declining at the world's highest juniper shrublines on the Tibetan Plateau. *Ecology* **2019**, *100*, e02557. [\[CrossRef\]](#)
7. Arekhi, M.; Yesil, A.; Ozkan, U.Y.; Balik Sanli, F. Detecting treeline dynamics in response to climate warming using forest stand maps and Landsat data in a temperate forest. *For. Ecosyst.* **2018**, *5*, 311–324. [\[CrossRef\]](#)
8. Marchand, W.; Girardin, M.P.; Hartmann, H.; Gauthier, S.; Bergeron, Y. Taxonomy, together with ontogeny and growing conditions, drives needleleaf species' sensitivity to climate in boreal North America. *Glob. Chang. Biol.* **2019**, *25*, 2793–2809. [\[CrossRef\]](#)
9. Alvarez, C.; Veblen, T.T.; Christie, D.A.; González-Reyes, A. Relationships between climate variability and radial growth of *Nothofagus pumilio* near altitudinal treeline in the Andes of northern Patagonia, Chile. *For. Ecol. Manag.* **2015**, *342*, 112–121. [\[CrossRef\]](#)
10. Huang, R.; Zhu, H.F.; Liang, E.Y.; Liu, B.; Shi, J.F.; Zhang, R.B.; Yuan, Y.J.; Griesinger, J. A tree ring-based winter temperature reconstruction for the southeastern Tibetan Plateau since 1340 CE. *Clim. Dyn.* **2019**, *53*, 3221–3233. [\[CrossRef\]](#)
11. Yu, D.; Wang, Q.; Wang, Y.; Zhou, W.; Hong, D.; Fang, X.; Jiang, S.; Dai, L. Climatic effects on radial growth of major tree species on Changbai Mountain. *Ann. For. Sci.* **2011**, *68*, 921–933. [\[CrossRef\]](#)
12. Zhang, Y.; Yin, D.C.; Sun, M.; Wang, H.; Tian, K.; Xiao, D.R.; Zhang, W.G. Variations of climate-growth response of major conifers at upper distributional limits in Shika Snow Mountain, Northwestern Yunnan Plateau, China. *Forests* **2017**, *8*, 377. [\[CrossRef\]](#)
13. Lamarche, V.C. *Frequency-Dependent Relationships between Tree-Ring Series along an Ecological Gradient and Some Dendroclimatic Implications*; CiteSeer: Princeton, NJ, USA, 1974.
14. Dittmar, C.; Zech, W.; Elling, W. Growth variations of Common beech (*Fagus sylvatica* L.) under different climatic and environmental conditions in Europe—a dendroecological study. *For. Ecol. Manag.* **2003**, *173*, 63–78. [\[CrossRef\]](#)
15. Leal, S.; Melvin, T.M.; Grabner, M.; Wimmer, R.; Briffa, K.R. Tree-ring growth variability in the Austrian Alps: The influence of site, altitude, tree species and climate. *Boreas* **2007**, *36*, 426–440. [\[CrossRef\]](#)
16. Liu, L.S.; Shao, X.M.; Liang, E.Y. Climate Signals from Tree Ring Chronologies of the Upper and Lower Treelines in the Dulan Region of the Northeastern Qinghai-Tibetan Plateau. *J. Integr. Plant Biol.* **2010**, *48*, 278–285. [\[CrossRef\]](#)
17. Liang, E.Y.; Wang, Y.F.; Xu, Y.; Liu, B.M.; Shao, X. Growth variation in *Abies georgei* var. *smithii* along altitudinal gradients in the Sygera Mountains, southeastern Tibetan Plateau. *Trees* **2010**, *24*, 363–373. [\[CrossRef\]](#)
18. Fan, Z.X.; Bräuning, A.; Thomas, A.; Li, J.B.; Cao, K.F. Spatial and temporal temperature trends on the Yunnan Plateau (Southwest China) during 1961–2004. *Int. J. Climatol.* **2011**, *31*, 2078–2090. [\[CrossRef\]](#)
19. Bräuning, A. Dendrochronology for the last 1400 years in eastern Tibet. *Geojournal* **1994**, *34*, 75–95. [\[CrossRef\]](#)
20. Zhang, Q.B.; Cheng, G.D.; Yao, T.D.; Kang, X.C.; Huang, J.G. A 2326-year tree-ring record of climate variability on the Northeastern Qinghai-Tibetan Plateau. *Geophys. Res. Lett.* **2003**, *30*, HLS 2-1. [\[CrossRef\]](#)
21. Fan, Z.X.; Bräuning, A.; Cao, K.F. Annual temperature reconstruction in the central Hengduan Mountains, China, as deduced from tree rings. *Dendrochronologia* **2008**, *26*, 97–107. [\[CrossRef\]](#)
22. Fan, Z.X.; Bräuning, A.; Cao, K.F. Tree-ring based drought reconstruction in the central Hengduan Mountains region (China) since A.D. 1655. *Int. J. Climatol.* **2010**, *28*, 1879–1887. [\[CrossRef\]](#)
23. Fan, Z.X.; Bräuning, A.; Cao, K.F.; Zhu, S.D. Growth-climate responses of high-elevation conifers in the central Hengduan Mountains, southwestern China. *For. Ecol. Manag.* **2009**, *258*, 306–313. [\[CrossRef\]](#)
24. Li, Z.S.; Zhang, Q.B.; Ma, K. Tree-ring reconstruction of summer temperature for A.D. 1475–2003 in the central Hengduan Mountains, Northwestern Yunnan, China. *Clim. Chang.* **2012**, *110*, 455–467. [\[CrossRef\]](#)
25. Panthi, S.; Bräuning, A.; Zhou, Z.K.; Fan, Z.X. Growth response of *Abies georgei* to climate increases with elevation in the central Hengduan Mountains, southwestern China. *Dendrochronologia* **2018**, *47*, 1–9. [\[CrossRef\]](#)
26. Guo, G.; Li, Z.S.; Zhang, Q.B.; Ma, K.P.; Mu, C. Dendroclimatological studies of *Picea likiangensis* and *Tsuga dumosa* in Lijiang, China. *IAWA J.* **2009**, *30*, 435–441. [\[CrossRef\]](#)
27. Bi, Y.F.; Xu, J.C.; Gebrekirstos, A.; Guo, L.; Zhao, M.X.; Liang, E.Y.; Yang, X.F. Assessing drought variability since 1650 AD from tree-rings on the Jade Dragon Snow Mountain, southwest China. *Int. J. Climatol.* **2016**, *35*, 4057–4065. [\[CrossRef\]](#)
28. Zhang, Y.; Cao, R.J.; Yin, J.; Tian, K.; Zhang, W.G.; Yin, D.C. Radial growth response of major conifers to climate change on Haba Snow Mountain, Southwestern China. *Dendrochronologia* **2020**, *60*, 125682. [\[CrossRef\]](#)
29. Yin, D.C.; Xu, D.R.; Tian, K.; Xiao, D.R.; Zhang, W.G.; Sun, D.C.; Sun, H.; Zhang, Y. Radial growth response of *Abies georgei* to climate at the Upper timberlines in Central Hengduan Mountains, Southwestern China. *Forests* **2018**, *9*, 606. [\[CrossRef\]](#)
30. Liu, G.; Zhang, W.; He, M.Y. The preliminary study of quaternary glacier development in Haba snow mountain. *Yunnan Geogr. Environ. Res.* **2012**, *24*, 104–110.
31. Su, H.; Wang, P. Climate vertical zoning of Haba natural reserve. *Yunnan Geogr. Environ. Res.* **2011**, *23*, 47–51.
32. Stokes, M.A.; Smiley, T.L. *An Introduction to Tree-Ring Dating*; University of Arizona Press: Tucson, AZ, USA, 1996.
33. Larsson. CooRecorder and CDendro Programs of the CooRecorder/CDendro Package Version 9.3. 2019. Available online: <http://www.cybis.se/forfun/dendro/> (accessed on 11 July 2017).
34. Holmes, R.L. Computer-assisted quality control in tree-ring Dating and Measurement. *Tree-Ring Bull.* **1983**, *43*, 69–75.
35. Vicente-Serrano, S.M.; Beguería, S.; López-Moreno, J.I. A multiscalar drought index sensitive to global warming: The standardized precipitation evapotranspiration index. *J. Clim.* **2010**, *23*, 1696–1718. [\[CrossRef\]](#)
36. Oberhuber, W. Influence of climate on radial growth of *Pinus cembra* within the alpine timberline ecotone. *Tree Physiol.* **2004**, *24*, 291–301. [\[CrossRef\]](#)

37. Biondi, F.; Waikul, K. DENDROCLIM2002: A C++ program for statistical calibration of climate signals in tree-ring chronologies. *Comput. Geosci.* **2004**, *30*, 303–311. [\[CrossRef\]](#)
38. Ter Braak, C.J.; Smilauer, P. *CANOCO Reference Manual and CanoDraw for Windows User's Guide: Software for Canonical Community Ordination (Version 4.5)*; Microcomputer Power: Ithaca, NY, USA, 2002.
39. Gaire, N.P.; Fan, Z.X.; Braeuning, A.; Panthi, S.; Rana, P.; Shrestha, A.; Bhujju, D.R. *Abies spectabilis* shows stable growth relations to temperature, but changing response to moisture conditions along an elevation gradient in the central Himalaya. *Dendrochronologia* **2020**, *60*, 125675. [\[CrossRef\]](#)
40. Rai, S.; Dawadi, B.; Wang, Y.F.; Lu, X.M.; Sigdel, S.R. Growth response of *Abies spectabilis* to climate along an elevation gradient of the Manang valley in the central Himalayas. *J. For. Res.* **2020**, *31*, 2245–2254. [\[CrossRef\]](#)
41. Denmead, O.T.; Shaw, R.H. Availability of soil water to plants as affected by soil moisture content and meteorological conditions 1. *Agron. J.* **1962**, *54*, 385–390. [\[CrossRef\]](#)
42. Griesinger, J.; Bräuning, A. Late Holocene variations in monsoon intensity in the Tibetan Himalayan Region-Evidence from tree rings. *J. Geol. Soc. India* **2006**, *68*, 485–493.
43. Li, J.B.; Shi, J.F.; Zhang, D.D.; Yang, B.; Fang, K.Y.; Yue, P.H. Moisture increase in response to high-altitude warming evidenced by tree-rings on the southeastern Tibetan Plateau. *Clim. Dyn.* **2017**, *48*, 649–660. [\[CrossRef\]](#)
44. Liang, E.Y.; Dawadi, B.; Pederson, N.; Eckstein, D. Is the growth of birch at the upper timberline in the Himalayas limited by moisture or by temperature? *Ecology* **2014**, *95*, 2453–2465. [\[CrossRef\]](#)
45. Dawadi, B.; Liang, E.Y.; Tian, L.D.; Devkota, L.P.; Yao, T.D. Pre-monsoon precipitation signal in tree rings of timberline *Betula utilis* in the central Himalayas. *Quat. Int.* **2013**, *283*, 72–77. [\[CrossRef\]](#)
46. Kharal, D.K.; Thapa, U.K.; George, S.S.; Meilby, H.; Rayamajhi, S.; Bhujju, D.R. Tree-climate relations along an elevational transect in Manang Valley, central Nepal. *Dendrochronologia* **2017**, *41*, 57–64. [\[CrossRef\]](#)
47. Sohar, K.; Altman, J.; Lehečková, E.; Doležal, J. Growth-climate relationships of Himalayan conifers along elevational and latitudinal gradients. *Int. J. Climatol.* **2017**, *37*, 2593–2605. [\[CrossRef\]](#)
48. Wang, H.; Zhou, J.; Qin, X.H.; Zhang, Y. Radial Growth Responses of *Pinus densata* to Climate Change in Haba Snow Mountain, Southwest China. *For. Resour. Manag.* **2019**, *2*, 67–72. (In Chinese)
49. Liang, E.Y.; Shao, X.M.; Xu, Y. Tree-ring evidence of recent abnormal warming on the southeast Tibetan Plateau. *Theor. Appl. Climatol.* **2009**, *98*, 9–18. [\[CrossRef\]](#)
50. Cannell, M.G.R. Growth control in woody plants. *Tree Physiol.* **1997**, *17*, 489. [\[CrossRef\]](#)
51. Büntgen, U.; Frank, D.C.; Kaczka, R.J.; Verstege, A.; Zwijacz-Kozica, T.; Esper, J. Growth responses to climate in a multi-species tree-ring network in the Western Carpathian Tatra Mountains, Poland and Slovakia. *Tree Physiol.* **2007**, *27*, 689–702. [\[CrossRef\]](#) [\[PubMed\]](#)
52. Gricar, J.; Zupancic, M.; Cufar, K.; Oven, P. Regular cambial activity and xylem and phloem formation in locally heated and cooled stem portions of Norway spruce. *Wood Sci. Technol.* **2007**, *41*, 463–475. [\[CrossRef\]](#)
53. Takahashi, K.; Okuhara, I.; Tokumitsu, Y.; Yasue, K. Responses to climate by tree-ring widths and maximum latewood densities of two *Abies* species at upper and lower altitudinal distribution limits in central Japan. *Trees-Struct. Funct.* **2011**, *25*, 745–753. [\[CrossRef\]](#)
54. Zhang, Y.; Yin, D.C.; Zhang, W.G.; Yue, H.T.; Du, J.C.D.; Li, Q.P.; Yang, R.; Tian, K. Response of radial growth of two conifers to temperature and precipitation in Potatso National Park, Southwest China. *Acta Ecol. Sin.* **2018**, *38*, 5383–5392. (In Chinese)
55. Qin, L.; Yuan, Y.; Zhang, R.; Wei, W.; Yu, S.; Fan, Z.; Chen, F.; Zhang, Y.; Shang, H. Tree-ring response to snow cover and reconstruction of century annual maximum snow depth for Northern Tianshan Mountains, China. *Geochronometria* **2016**, *43*, 9–17. [\[CrossRef\]](#)
56. Villalba, R.; Boninsegna, J.; Veblen, T.T.; Schmelter, A.; Rubulis, S. Recent trends in tree-ring records from high elevation sites in the Andes of northern Patagonia. *Clim. Chang.* **1997**, *36*, 425–454. [\[CrossRef\]](#)
57. Vaganov, E.A.; Hughes, M.K.; Kirdyanov, A.V.; Schweingruber, F.H.; Silkin, P.P. Influence of snowfall and melt timing on tree growth in Subarctic Eurasia. *Nature* **1999**, *400*, 149–151. [\[CrossRef\]](#)
58. Yu, D.; Wang, G.G.; Dai, L.; Wang, Q. Dendroclimatic analysis of *Betula ermanii* forests at their upper limit of distribution in Changbai Mountain, Northeast China. *For. Ecol. Manag.* **2007**, *240*, 105–113. [\[CrossRef\]](#)
59. Takahashi, K.; Tokumitsu, Y.; Yasue, K. Climatic factors affecting the tree-ring width of *Betula ermanii* at the timberline on Mount Norikura, central Japan. *Ecol. Res.* **2005**, *20*, 445–451. [\[CrossRef\]](#)
60. Payette, S.; Delwalde, A.; Morneau, C.; Lavole, C. Patterns of tree stem decline along a snow-drift gradient at treeline: A case study using stem analysis. *Can. J. Bot.* **1998**, *74*, 1671–1683. [\[CrossRef\]](#)
61. Liang, E.Y.; Shao, X.M.; Hu, Y.X.; Lin, J.X. Dendroclimatic evaluation of climate-growth relationships of Meyer spruce (*Picea meyeri*) on a sandy substrate in semi-arid grassland, north China. *Trees-Struct. Funct.* **2001**, *15*, 230–235. [\[CrossRef\]](#)